Power regulation in pitch-controlled variable-speed WECS above rated wind speed

F.D.Bianchi * R.J.Mantz † C.F.Christiansen ‡

Laboratorio de Electrónica Industrial, Control e Instrumentación (LEICI), Facultad de Ingeniería, Universidad Nacional de La Plata, CC 91, 1900 La Plata, Argentina

Abstract

In medium to large scale wind energy conversion systems (WECS), the control of the pitch angle of the blades is an usual method for power regulation above rated wind speed. However, limitations of the pitch actuator have a marked influence on the regulation performance. In variable-speed mode the control of the generator torque is able to reduce the effects of the pitch actuator limitations. Nevertheless, in this case the system is Multiple-Input Multiple-Output (MIMO) and then the control design results more complex. In this situation advance control techniques, such as optimal control, are an interesting option for a systematic controller design. This work analyzes variable-pitch power regulation above rated wind speed in the context of optimal control. The analysis is approached from a new point of view in order to establish a clear connection between the choice of the optimization criteria and the compromise between power regulation and pitch actuator limitations.

Keywords: Wind energy conversion systems, pitch control, variable-speed.

1 Introduction

Wind energy conversion systems (WECS) present two operating modes according to how the wind turbine is connected to the grid [1]. In fixed-speed mode the turbine is directly

*CONICET - UNLP. Corresponding author. Phone/Fax: +54 221 4259306. E-mail: fbianchi@ing.unlp.edu.ar

†CICpBA - UNLP

‡UNLP

connected to the grid, fixing the rotational speed to the grid frequency. In variable-speed mode an electronic converter is inserted between the generator and the grid [2, 3], or a doubly-fed induction generator (DFIG) controlled by the rotor circuit is used [4,5]. Thus, the rotational speed can change independently of the grid frequency.

Commonly, regulation objectives change according to the wind speed. In low speed it is aimed to capture energy as much as possible. Variable-speed mode is especially useful in this operating region since the electronic converter can maximize the conversion efficiency by controlling the generator torque. When the wind speed reaches some rated value, a limit on the power is needed to prevent the turbine overloading. Additionally, acoustic noise and other design constraints impose a rotational speed limit [1, 6].

There are several options depending on the operating mode to limit the power and the rotational speed. In fixed-speed mode, there exist both passive and active strategies to avoid exceeding the limits on power and speed. In passive strategies the blade design itself assures the turbine works within safe limits at any wind speed. Although these strategies are simple and inexpensive, they cause high stationary loads and loss of energy [1]. The active strategies consist in varying the pitch angle of the blades. The turbines with variable-pitch capability can modify the lift and hence the conversion efficiency. Even though variable-pitch methods are more expensive and more complex, they achieve a better power regulation and lower dynamic loads [1, 7]. In variable-speed mode it is possible to regulate the power and the rotational speed if the turbine is operated at low conversion efficiency [2, 5, 8, 9]. However, in this last situation may arise some stability problems [9, 10].

Nowadays there exists an increasing interest in control of pitch-controlled variable-speed WECS above rated wind speed [6, 7, 10, 11]. This combination aims to compensate the limitations of each strategy (variable-pitch and variable-speed) working independently. The ability to regulate power of the pitch control is limited by the pitch rate. The control of generator torque is fast, but when it is applied to limit the power and the speed, stability problems may arise. When both controls works together, they may improve the transient response while the stability problems are avoided.

WECS with the capability to change both the rotational speed and the pitch angle are Multiple-Input Multiple-Output (MIMO) systems with strongly coupled variables. Consequently, the control design results more complex than the other cases. For this reason, many of the strategies proposed in the literature adjust independently each control

variable. For instances, some strategies only apply pitch control above rated wind speed (variable-speed mode is used below rated wind speed for energy capture maximization) [6, 11]. Other strategies control simultaneously the generator torque and the pitch angle, but the controllers are designed separately [10]. In order to consider the coupling between variables, more advance techniques, such as optimal control, are required.

This paper studies, in the context of optimal control, the power regulation above rated wind speed. Both limitations of fixed-speed strategies and potential improvements of variable-speed controls are investigated. Based on this analysis, it is established a clear connection between optimization criteria and the compromise between power regulation and limited pitch rate.

2 System description

Figure1 depicts a block diagram of a WECS configuration with the capability to change the rotational speed and the pitch angle.

The subsystem named "aerodynamics" converts the kinetic energy of the wind into mechanical energy. The inputs are the wind speed V, the pitch angle β, and the turbine rotational speed Ω_r. The output is the aerodynamic torque:

$$T_r(V, \beta, \Omega_r) = \frac{\pi \rho R^2 C_p(\lambda, \beta)}{2\lambda} V^2 \tag{1}$$

where ρ is the air density, R is the rotor radius, λ is the tip-speed ratio ($\lambda = \Omega_r R/V$), and $C_p(\cdot)$ is the power coefficient which indicates the turbine efficiency to convert the wind energy into useful mechanical energy. Figure 2 presents a typical power coefficient as function of λ and β where the point of maximum conversion efficiency is indicated with $C_p(\lambda_o, \beta_o)$ [1].

The "pitch actuator" block represents the mechanical and hydraulic system that rotates the blades around their longitudinal axis. This subsystem is described as a first order model with saturation limits on β and the pitch rate $\dot{\beta}$ [7].

The "generation unit" converts the mechanical energy supplied by the wind turbine into electrical energy. This subsystem includes the electrical generator and, in the case of variable-speed WECS, an electronic converter. Commonly, the dynamics of the generation unit is much faster than those of the other blocks, and then it can be neglected. Therefore, assuming small slip and constant magnetic flux, the generator torque can be expressed as

$$T_g = c_1 \Omega_g + c_2 \mu \tag{2}$$

where c_1 and c_2 are constant coefficients and μ is the control input (μ is the synchronic frequency in squirrel-cage configurations or the control signal of the converter in DFIG configurations).

Finally, the "mechanics" subsystem describes the drive-train dynamics (rotor, generator, and gearbox). Normally, to represent the resonant modes found in WECS, this system is modeled as a series of inertias joined with flexible shafts with friction. The complexity of the model depends on the particular system. If the turbine is very flexible, more resonant modes must be considered, and the model will be more complex [2].

The resulting interconnection of the previous subsystems is a highly nonlinear system due to the expression of the aerodynamic torque (1). Nevertheless, for a local analysis the expression (1) can be linearized

$$\hat{T}_r = k_{\Omega_r}\hat{\Omega}_r + k_V\hat{V} + k_\beta\hat{\beta} \tag{3}$$

where $k_{\Omega_r} = \partial T_r/\partial\Omega_r$, $k_V = \partial T_r/\partial V$, and $k_\beta = \partial T_r/\partial\beta$ are functions of the operating point, and the variables with $\hat{}$ correspond to deviations from the operating point. Then, considering a third order model for the mechanical subsystem [7], the linearized model results

$$\dot{\hat{x}} = \begin{bmatrix} 0 & 1 & -1 & 0 \\ -K_s/J_r & (k_{\Omega_r} - B_s)/J_r & B_s/J_r & k_\beta/J_r \\ K_s/J_g & B_s/J_g & (-c_1 - B_s)/J_g & 0 \\ 0 & 0 & 0 & -\tau \end{bmatrix} \hat{x} + \begin{bmatrix} 0 & 0 & 0 \\ k_V/J_r & 0 & 0 \\ 0 & -c_2/J_g & 0 \\ 0 & 0 & 1 \end{bmatrix} \begin{bmatrix} \hat{V} \\ \mu \\ \beta_r \end{bmatrix} \tag{4}$$

where $x = \begin{bmatrix} \hat{\theta}_e & \hat{\Omega}_r & \hat{\Omega}_g & \hat{\beta} \end{bmatrix}^T$, $\hat{\theta}_e = \int(\hat{\Omega}_r - \hat{\Omega}_g)dt$, β_r is the pitch actuator input, τ is the time constant of the actuator, J_r and J_g are the moments of inertia of the wind turbine and the generator respectively, K_s is the stiffness coefficient, and B_s is the friction coefficient.

3 Power regulation in pitch-controlled WECS above rated wind speed

3.1 Fixed-speed mode

It can be inferred from the expression of the aerodynamic power

$$P_r = \frac{\pi\rho R^2}{2} C_p(\lambda, \beta) V^3 \tag{5}$$

that the part of the available wind power ($\frac{\pi\rho R^2}{2}V^3$) converted into useful mechanical power is determined by $C_p(\cdot)$. This coefficient can be interpreted as a variable gain controlled

by λ and β. Thus, below rated wind speed the power coefficient is maintained at the optimal value for energy capture maximization whereas above rated wind speed, where the turbine overloading must be avoided, the regulation objective requires a power coefficient reduction.

The power coefficient reduction is accomplished increasing β, decreasing λ, or changing both variables. In fixed-speed mode β is increased and Ω_r is fixed, i.e. λ is reduced as a result of the wind speed increment. Commonly, variable-pitch strategies are associated with good power regulation in steady state and low dynamic loads. However, the actuator constraints on β and $\dot{\beta}$ may deteriorate the transient response [11].

The effect of the pitch actuator limitations on the transient response can be evaluated by considering several restrictions on the pitch rate and the torque error. Optimal control theory provides a suitable framework for this analysis. In particular, $\mathcal{H}_\infty$ optimal control is applied since it does not require of disturbance modeling. Notice that due to the non-linear behavior of WECS, the considered control strategies are only valid in a local range. However, the local controllers can be interpolated by using gain scheduling techniques, and thus it is obtained a control law for the whole above rated region [12].

Figure 3 depicts the feedback diagram used to design the $\mathcal{H}_\infty$ optimal control for power regulation, where y is the generator torque, u is the pitch angle and $e = T_{nom} - T_g$. The input μ in (4) has not been indicated since, in this case, it is constant. In order to separate the control input β_r from the disturbance $\hat{V}$, the transfer of the system (4) is divided in the following way

$$\hat{T}_g = P_1\hat{V} + P_2\beta_r.$$

The transfers

$$W_e(s) = \frac{\rho_1}{s}, \tag{6}$$

$$W_u(s) = \frac{10s}{s+\rho_3} \tag{7}$$

introduce the objectives into the optimization problem.

The function $W_e(s)$[1] forces zero steady state error to maintain the generated power close to the rated limit P_{nom}. The transfer $W_u(s)$ allows β to reject the low frequency disturbances and penalizes the high frequency components to avoid the saturation of $\dot{\beta}$.

[1] In fact, in order to satisfy detectability and stabilizability conditions, $W_e(s)$ is factorized in $\tilde{W}_e(s)M(s)$ where $M(s)$ contains the integral action and $\tilde{W}_e(s)$ is stable and minimum phase [13].

Clearly, the controller design is a mixed sensitivity problem [13] where

$$\left\| \begin{array}{c} W_e S P_1 \\ W_u C S P_1 \end{array} \right\|_\infty \tag{8}$$

must be minimized, being S the sensitivity function defined as $S = (I + P_2 C)^{-1}$ and $\|\cdot\|_\infty$ the infinity norm.

Figure 4 presents simulations of the closed loop system with controllers designed for three different constraints on $\dot{\beta}$, i.e. three different ρ_3. The simulations correspond to a change in wind speed from 16 m/s to 17 m/s in 1 s. Note that as the constraint on $\dot{\beta}$ becomes stronger (i.e. ρ_3 is lower), the power regulation is deteriorated. It can also be observed the small change in Ω_g due to the high slope of generator torque curve.

The marked influence of the pitch rate on the power regulation results clear from Figure 5. This figure shows, on the torque-speed plane, the generator (thick line) and the aerodynamic (thin lines) torque curves for a pitch-controlled fixed-speed strategy. The curve **a** is the aerodynamic torque for a wind speed V_1 and a pitch angle β_1. The operating point **A**, where the curve **a** intersects the generator torque characteristic, corresponds to the nominal power P_{nom} and the nominal turbine speed Ω_{rnom}. The curves **b** is the aerodynamic torque for $V_2 > V_1$ and β_1, and the curve **c** is for V_2 and $\beta_2 > \beta_1$. The value β_2 assures the turbine works at **A** when the wind speed is V_2. As the pitch angle can not instantaneously be changed, a suddenly change in the wind speed ($V_1 \rightarrow V_2$) will produce the deviations of both power ($P_{nom} \rightarrow P_2$) and rotational speed ($\Omega_{rnom} \rightarrow \Omega_2$) observed in Figure 4. The deviations will return to zero when β reaches the value β_2.

3.2 Variable-speed mode

From an energy point of view, an increment on the wind speed lead to a power excess that must be discarded to avoid the turbine overloading. With this purpose, the fixed-speed strategy suits the turbine gain ($C_p(\cdot)$) to maintain the power constant. However, due to the limited pitch rate, a temporal increment on power is inevitable. Clearly, if the power excess is dissipated in someway, the power regulation will improve. That is, damping must be added.

Considering the third row in (4),

$$\dot{\hat{\Omega}}_g = \frac{K_s}{J_g}\hat{\theta}_e + \frac{B_s}{J_g}(\hat{\Omega}_r - \hat{\Omega}_g) - c_1\hat{\Omega}_g - c_2\mu,$$

it is clear that the system becomes more damping if the slope of the generator torque curve c_1 is lower. Obviously, a reduction in c_1 is unacceptable because it is equivalent to degrade the generator efficiency. Actually, this can be avoided in variable-speed mode with a suitable generator torque control. For instance, a control law $\mu = c_3\Omega_g$ applied in (2) results in the following torque expression

$$T_g = (c_1 + c_2c_3)\Omega_g$$

where c_3 is chosen to reduce the slope of the incremental generator torque characteristic (incremental slope for short).

If the concept of change in the incremental slope is included in the feedback diagram in Figure 3, it is possible to obtain a MIMO controller that considers the coupling among the different variables. The simultaneous use of β_r and μ allows a reduction in the incremental slope and an improvement on power regulation. Moreover, the optimization algorithm itself finds the most suitable incremental slope to achieve a compromise between power regulation and the allowable maximum pitch rate.

In order to introduce the concept of change in the incremental slope, $P_1(s)$ and $P_2(s)$ are redefined with the following input-output relationship

$$\begin{bmatrix} \hat{\Omega}_g \\ \hat{T}_g \end{bmatrix} = P_1\hat{V} + P_2 \begin{bmatrix} \mu \\ \beta_r \end{bmatrix}$$

where P_1 and P_2 are now transfer matrices.

In this case, the weighting functions are replaced with the following ones

$$W_e(s) = \begin{bmatrix} \rho_1 & 0 \\ 0 & \rho_2 \end{bmatrix} \frac{1}{s}, \tag{9}$$

$$W_u(s) = \begin{bmatrix} 0 & 0 \\ 0 & 10 \end{bmatrix} \frac{s}{s+\rho_3}. \tag{10}$$

The integral action in $W_e(s)$, as well as in the fixed-speed case, aims to achieve zero steady state error. The parameter ρ_1 and ρ_2 allow imposing different constrains on the errors of Ω_g and T_g, and thus they determine the slope of the incremental generator torque curve. The transfer $W_u(s)$ limits the derivative of the pitch angle.

Figure 6 presents simulations of the closed loop system with three controllers designed for $\rho_1 = 10$, $\rho_3 = 100$ and three different ρ_2. With the aim of comparison, it is also included the response of the closed loop system with the previously designed fixed-speed controller

corresponding to $\rho_1 = 0.1$ and $\rho_3 = 100$ (solid lines) in Figure 6. Clearly, Figure 6 reflects the effect of the change in the incremental slope on the power. When ρ_2 increases with fixed ρ_1, the incremental slope becomes lower, and then the power overshoot is decreased. It is interesting to note that when the constraint on Ω_g is too strong, the incremental slope can become higher than c_1, and then the power regulation results worse than in the fixed-speed case (dashed line). Note also that a higher change in Ω_g involves a higher $T_r - T_g$, i.e. an increment on dynamic loads. Additionally, it can be observed that $\dot{\beta}$ slightly increases when the incremental slope decreases. This fact is due to a lower gain at the transfer $\beta_r \rightarrow T_g$. However, in all cases $\dot{\beta}$ is within allowable limits.

Figure 7, as Figure 4, shows simulations of the closed loop systems with controllers designed for different constrains on the control input but with lower incremental slopes ($\rho_1 = 10$ and $\rho_2 = 0.1$). Again, it can be seen the compromise between power regulation and allowable pitch rate. If the constraint on the pitch rate is incremented, the power overshoot is higher, but it is always lower than in fixed-speed case. The higher changes in Ω_g reflects the lower slope of the incremental generator torque characteristic.

Finally, Figure 8 compares fixed-speed mode with variable-speed mode on the Ω_g-T_g plane. The simulations correspond to turbulent wind with a mean speed of 16 m/s. The line **a** is the response of the fixed-speed system, and the straight line **b** is an average response of the variable-speed system. The change in the slope is clear. The fixed-speed system works in the static curve $c_1\Omega_g + c_2\mu$ while the variable-speed system works in the incremental curve **b**, with a considerably lower slope.

4 Conclusions

In this paper the power regulation above rated wind speed in pitch-controlled WECS has been analyzed in the context of optimal control. In fixed-speed mode, the maximum pitch rate and the slope of the generator torque characteristic have a marked influence on the power response. In variable-speed mode, the effect of the generator torque control can be considered as a change in the slope of the incremental generator torque characteristic. Based on these facts, the choice of the optimization criteria are presented as a compromise between the power regulation and incremental slope. This new approach allows gaining an insight into the connections between the power regulation and the maximum allowable pitch rate and thus improving the controller design.

Acknowledgements

This work was supported by the Agencia Nacional para la Promoción Científica y Técnica ANPCyT, the Comisión de Investigaciones Científicas de la prov. de Buenos Aires CICpBA, the Consejo Nacional de Investigaciones Científicas y Técnicas CONICET and the Universidad Nacional de La Plata UNLP.

References

[1] L.L. Freris, editor. *Wind energy conversion systems*. Prentice Hall, 1990.

[2] T. Ekelund. *Modeling and linear quadratic optimal control of wind turbines*. PhD thesis, Chalmers Univ. of Techn., 1997.

[3] A. Miller, E. Muljadi, and D.S. Zinger. A variable speed wind turbine power control. *IEEE Trans. on Energy Conversion*, 12(2):181–186, June 1997.

[4] H. De Battista, P. Puleston, R.J. Mantz, and C.F. Christiansen. Sliding mode control of wind energy systems with DOIG-Power efficiency and torsional dynamics optimization. *IEEE Trans. on Power Systems*, 15(2):728–734, 2000.

[5] H. De Battista, R.J. Mantz, and C.F. Christiansen. Dynamical sliding mode power control of wind driven induction generators. *IEEE Trans. on Energy Conversion*, 15(4):451–457, 2000.

[6] E.A. Bossanyi. The design of closed loop controllers for wind turbines. *Wind Energy*, 3(3):149–163, 2000.

[7] X. Ma. *Adaptive extremum control and wind turbine control*. PhD thesis, Techn. Univ. of Denmark, 1997.

[8] E. Muljadi, K. Pierce, and P. Migliori. A conservative control strategy for variable-speed, stall-regulated wind turbine. In *Proc. of the 19th ASME Energy Symposium*, Reno, Nevada, 2000.

[9] H. De Battista, R.J. Mantz, and C.F. Christiansen. Performance analysis of a variable structure controller for power regulation of WECS operating in stall region. *International Journal of Energy Research*, 25:1345–1357, 2001.

[10] W.E. Leithead and B. Connor. Control of variable speed wind turbines: design task. *Int. Journal of Control*, 73(13):1189–1212, 2000.

[11] E. Muljadi and C.P. Butterfield. Pitch-controlled variable-speed wind turbine generation. *IEEE Trans. on Industrial Applications*, 37(1):240–246, 2001.

[12] W.J. Rugh and J.S. Shamma. Research on gain scheduling. *Automatica*, 36:1401–1425, 2000.

[13] K. Zhou, J. Doyle, and K. Glover. *Robust and optimal control*. Prentice Hall, Upper Saddle River, New Jersey, 1996.

Figure Captions

Figure 1. Block diagram of a WECS configuration with the capability to change the rotational speed and the pitch angle.

Figure 2. Typical power coefficient $C_p(\lambda, \beta)$.

Figure 3. Feedback diagram for power regulation.

Figure 4. Closed loop simulations corresponding to a change in wind speed from 16 m/s to 17 m/s in 1 s for a pitch-controlled fixed-speed control strategy.

Figure 5. Fixed-speed power regulation on the torque-speed plane.

Figure 6. Closed loop simulations corresponding to a change in wind speed from 16 m/s to 17 m/s in 1 s for three different variable-speed controllers designed for different ρ_2 and a fixed-speed controller.

Figure 7. Closed loop simulations corresponding to a change in wind speed from 16 m/s to 17 m/s in 1 s for three different variable-speed controllers designed for different ρ_3.

Figure 8. Closed loop simulations corresponding to a turbulent wind with mean at 16 m/s on the Ω_g-T_g plane. **a**: fixed-pitch and **b**: variable-speed.

Figures

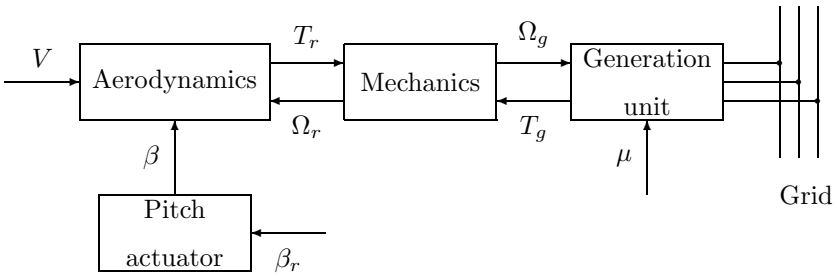

Figure 1: Block diagram of a WECS configuration with the capability to change the rotational speed and the pitch angle.

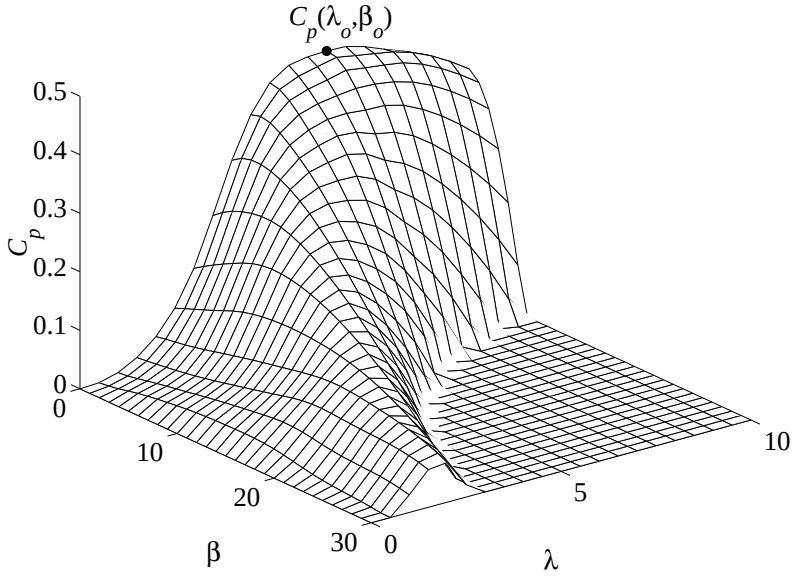

Figure 2: Typical power coefficient $C_p(\lambda, \beta)$.

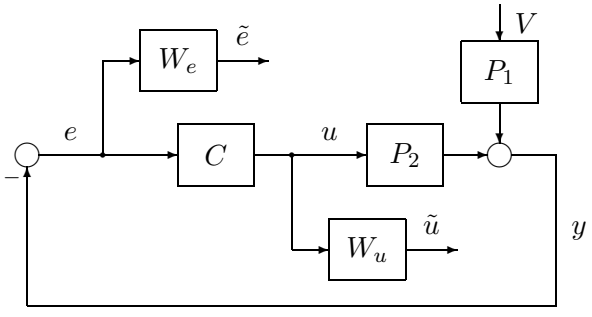

Figure 3: Feedback diagram for power regulation.

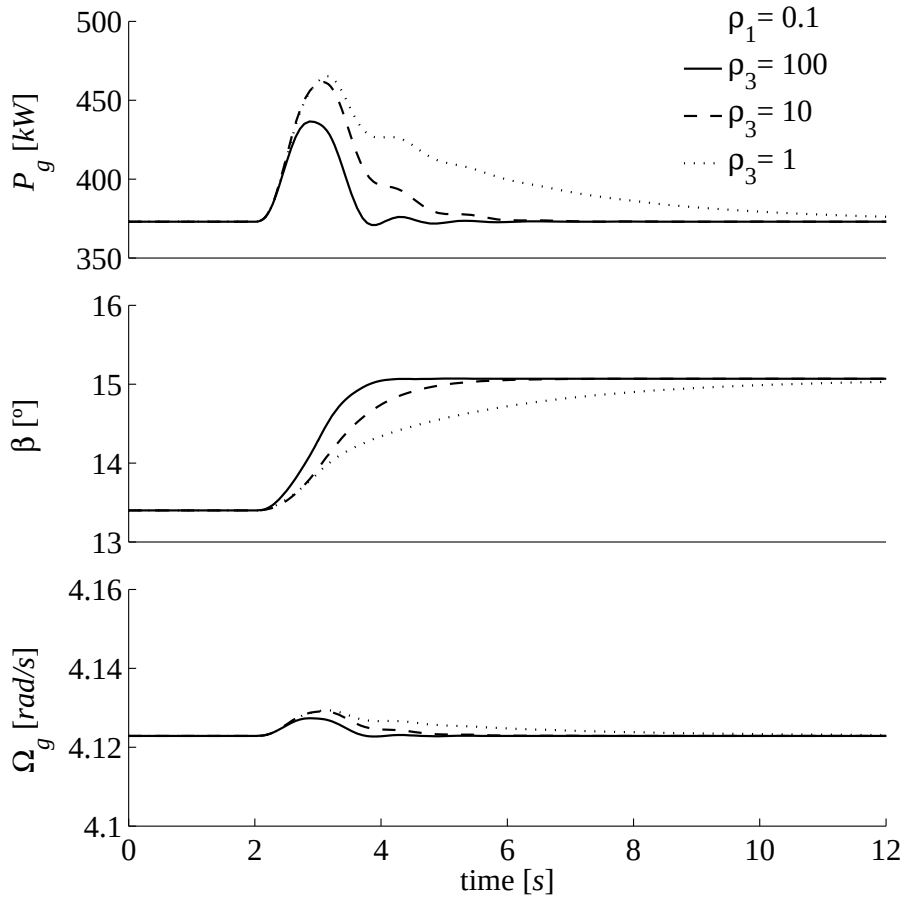

Figure 4: Closed loop simulations corresponding to a change in wind speed from 16 m/s to 17 m/s in 1 s for a pitch-controlled fixed-speed control strategy.

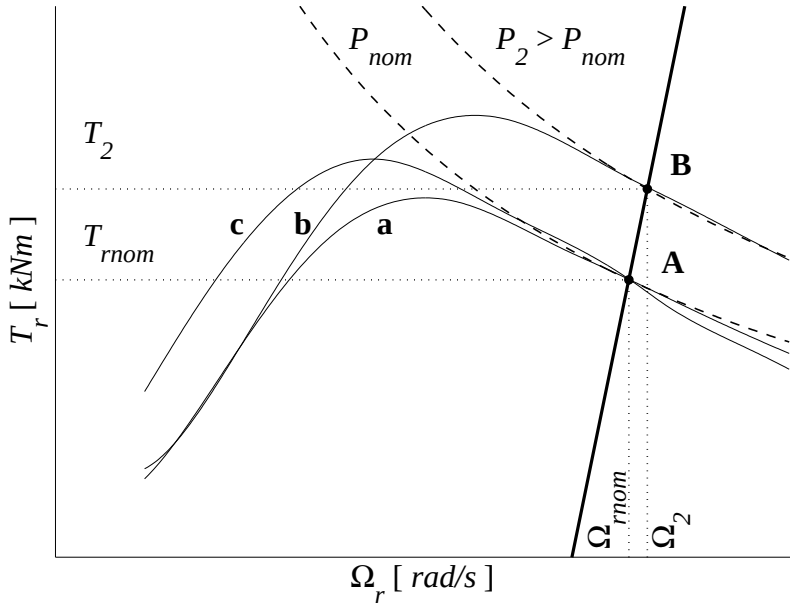

Figure 5: Fixed-speed power regulation on the torque-speed plane.

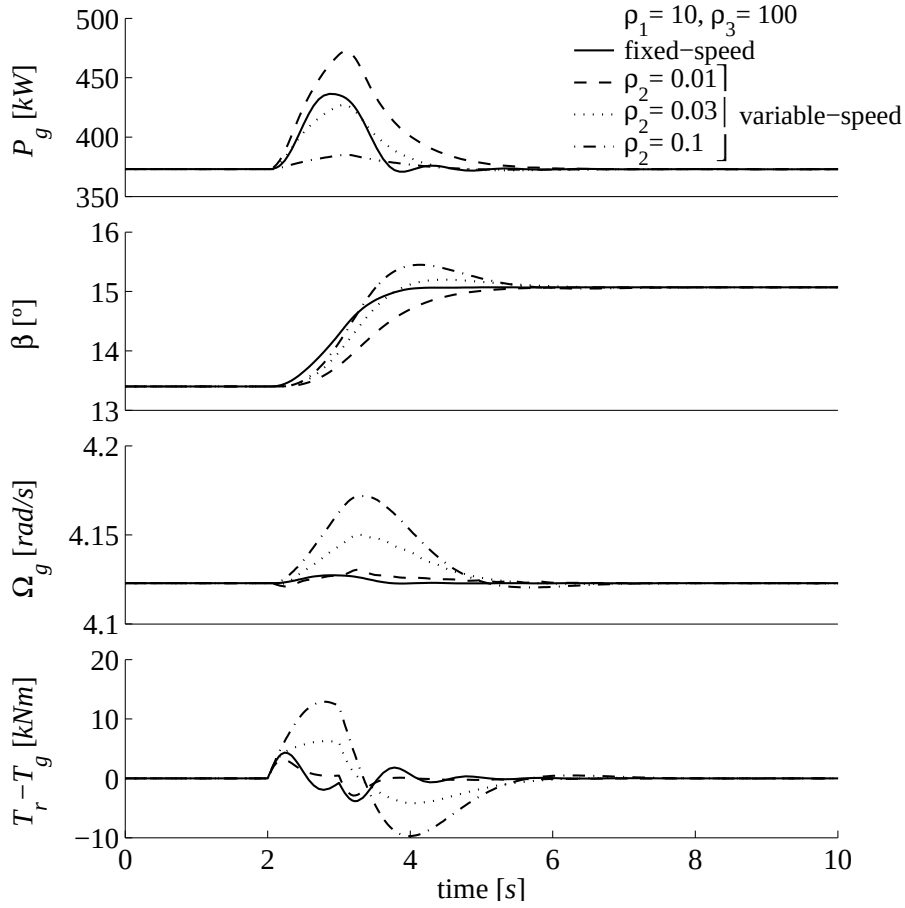

Figure 6: Closed loop simulations corresponding to a change in wind speed from 16 m/s to 17 m/s in 1 s for three different variable-speed controllers designed for different ρ_2 and a fixed-speed controller.

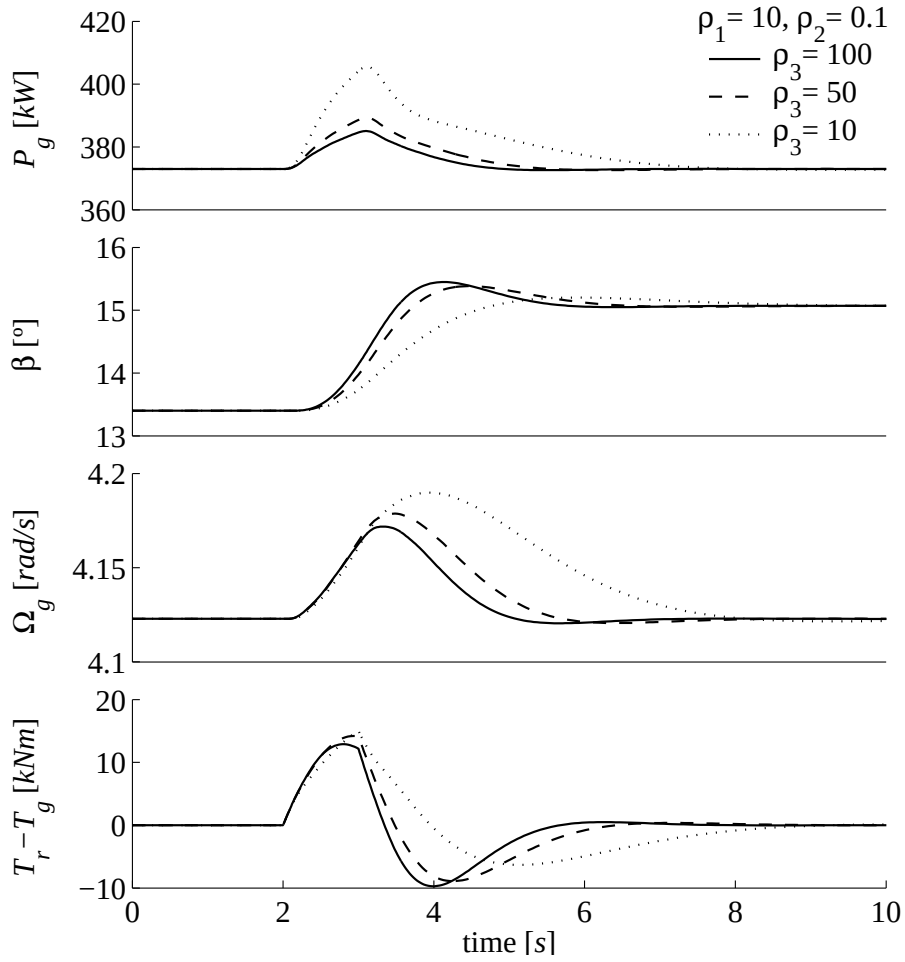

Figure 7: Closed loop simulations corresponding to a change in wind speed from 16 m/s to 17 m/s in 1 s for three different variable-speed controllers designed for different ρ_3.

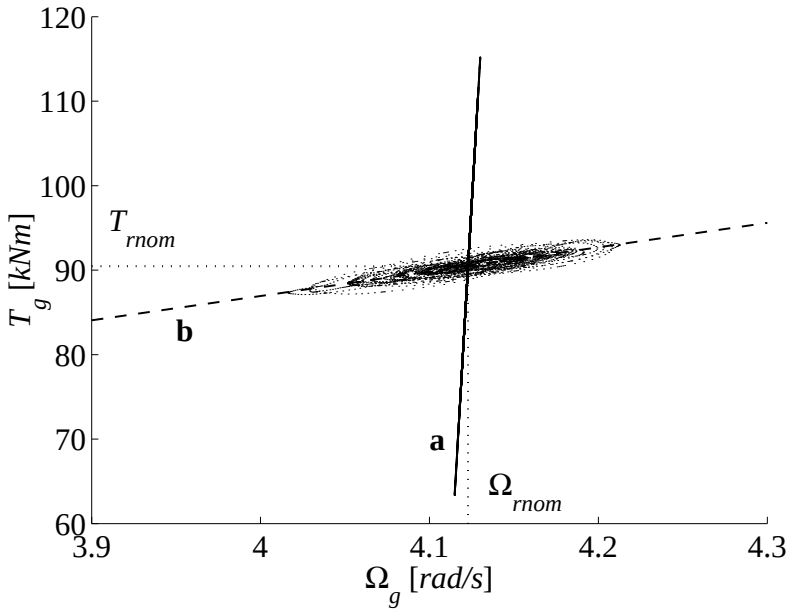

Figure 8: Closed loop simulations corresponding to a turbulent wind with mean at 16 m/s on the Ω_g-T_g plane. **a**: fixed-pitch and **b**: variable-speed.